Photoionization of calcium

Pranawa C. Deshmukh* and W. R. Johnson

Department of Physics, University of Notre Dame, Notre Dame, Indiana 46556

A study of the photoionization of calcium in the relativistic random-phase approximation is reported. Predictions of photoionization cross sections, angular distribution asymmetry parameters, and spin-polarization parameters for the $4s$, $3p$, and $3s$ subshells are made with emphasis on the energy region above the $3p_{3/2}$ threshold where multiconfigurational effects are not expected to be very important. Autoionization resonances below the $3s$ threshold and between the $3p_{3/2}$ and $3p_{1/2}$ thresholds are analyzed using the relativistic multichannel quantum-defect theory.

I. INTRODUCTION

The absorption of electromagnetic radiation by calcium has been of considerable interest[1-14] to physicists especially from the point of view of astrophysical processes.[9,11] Experimental data are available mainly in the uv region in the neighborhood of photon energies just above the threshold for ionization in the $4s$ subshell[7-11] and in the extreme uv region above the $2p$ threshold.[12] Excitation of the $3p$ subshell in the vacuum uv region has been reported,[13] and very recently, double photoionization in the same region has been studied.[14] The ground state of calcium is generally regarded as $[Ar]4s^2 {:}^1S_0$, but as one would expect there is considerable evidence for mixing from the low-lying $3d^2$ and $4p^2$ configurations. The configuration interaction complicates the photoionization spectrum in the energy region just above the $4s$ threshold, but plays a relatively less important role in the absorption process at much higher energies, for example, above the $3p$ ionization threshold. To study the photoabsorption by calcium, we have made use of the relativistic random-phase approximation (RRPA).[15-17] The RRPA accounts for many-body effects and also the relativistic interactions responsible for spin-orbit splitting. Although the unperturbed state is regarded in the RRPA as consisting only of a single configuration, the application of the RRPA has been taken up here in order to provide a framework for the development of a multiconfigurational RRPA study which will account also for the multiconfigurational nature of the ground state.

In the present work we study the photoionization of $4s$, $3p_{3/2}$, $3p_{1/2}$, and $3s$ subshells of calcium. In applying the RRPA, only the correlations emerging from the coupling between the channels obtained by

excitation of the subshells mentioned above were included (truncated RRPA). There are nine such channels permitted by dipole selection rules:

$$4s_{1/2} \rightarrow p_{1/2}, p_{3/2} \, ,$$

$$3p_{3/2} \rightarrow s_{1/2}, d_{3/2}, d_{5/2} \, ,$$

$$3p_{1/2} \rightarrow s_{1/2}, d_{3/2} \, ,$$

and

$$3s_{1/2} \rightarrow p_{1/2}, p_{3/2} \, .$$

The energy range covered is from the $3p_{1/2}$ threshold ($\simeq 1.35$ a.u.) to 10 a.u. Subshell cross sections, angular distribution asymmetry parameters, spin-polarization parameters for the $4s$, $3p$, and $3s$ shells and the branching ratio for the $3p$ shell are studied. Further, we have employed the multichannel quantum-defect theory[18] (MQDT) in the present investigation to explore photoionization properties in the sensitive regions where autoionization resonances occur.

The RRPA thresholds are the Dirac-Fock (DF) eigenvalues[15] which differ from the experimental thresholds because of the neglect of certain many-

TABLE I. Calculated Dirac-Fock (DF) and experimental values (in a.u.) of the thresholds for the outer subshells of calcium.

Subshell	DF	Experimental[a]
$4s$	0.196	0.22
$3p_{3/2}$	1.334	1.261
$3p_{1/2}$	1.349	1.276
$3s$	2.262	1.69

[a]Moore, Ref. 21.

body correlations.[19,20] The theoretical and the experimental thresholds are given in Table I.

II. CROSS SECTIONS
AND ANGULAR DISTRIBUTIONS

The differential cross section for photoionization of a subshell $n\kappa$ is given by[17,22]

$$\frac{d}{d\Omega}\sigma_{n\kappa} = \frac{\sigma_{n\kappa}(\omega)}{4\pi}[1 - \tfrac{1}{2}\beta_{n\kappa}(\omega)P_2(\cos\theta)] ,$$

(1)

where the partial cross section $\sigma_{n\kappa}$ for the subshell $n\kappa$ is given by[17]

$$\sigma_{n\kappa}(\omega) = \frac{4\pi^2\alpha\omega}{3}(|D_{nj\to j-1}|^2 + |D_{nj\to j}|^2 + |D_{nj\to j+1}|^2) .$$

(2)

FIG. 2. 3p subshell cross section above the $3p_{1/2}$ threshold.

In the above equations n refers to the principal quantum number and $\kappa = \mp(j+\tfrac{1}{2})$ for $j=l\pm\tfrac{1}{2}$, where j and l are the single electron total and orbital angular momentum quantum numbers. The RRPA reduced dipole matrix element for the photoionization channel $nj \to j'$ is denoted by $D_{nj\to j'}$ and the quantity $\beta_{n\kappa}(\omega)$ in Eq. (1) is the angular distribution asymmetry parameter for the subshell $n\kappa$ which can also be expressed in terms of the dipole amplitudes $D_{nj\to j'}$.[17]

The partial cross section for photoionization from the outermost 4s subshell of calcium in the energy range from the $3p_{1/2}$ threshold to 10 a.u. is shown in Fig. 1. The curve in Fig. 1 is discontinuous in the region slightly below the 3s threshold, since in that region the cross section has a complicated structure due to coupling between open and closed channels which lead to autoionization resonances converging to the 3s threshold. These resonances are discussed below using the MQDT.[18] The 4s cross section has a minimum at about 1.9 a.u. This is the second minimum in the 4s cross section

and is due to interchannel coupling; the first minimum appears just above the 4s threshold and is not shown in Fig. 1.

The partial cross section for the 3p shell is shown in Fig. 2, above the $3p_{1/2}$ threshold. Since the present calculation is relativistic, partial cross sections for the subshells $3p_{3/2}$ and $3p_{1/2}$ were obtained separately, but only the total 3p cross section is presented in Fig. 2. The nonrelativistic RPAE (random-phase approximation with exchange) calculation of Amusia et al.[23] practically coincides with the present results, though the present calculation leads to a somewhat lower value of the 3p cross section near the $3p_{1/2}$ threshold. The photoionization cross section calculated by McGuire[6] using an approximate Hartree-Fock-Slater potential in the region between the 3p and 3s thresholds is much lower than both the RRPA and RPAE results, but McGuire's results do show a broad peak in the neighborhood of 3 a.u. similar to that seen in Fig. 2. In the nonrelativistic limit one obtains for the branching ratio

$$\gamma = \sigma_{3p_{3/2}}/\sigma_{3p_{1/2}} ,$$

(3)
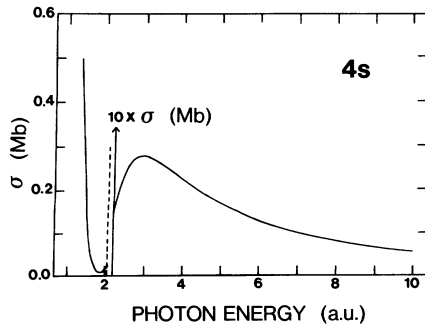
the statistical ratio of the relative occupation of the

FIG. 1. 4s subshell partial cross section above the $3p_{1/2}$ threshold. The region of autoionization resonances below the 3s threshold is omitted.
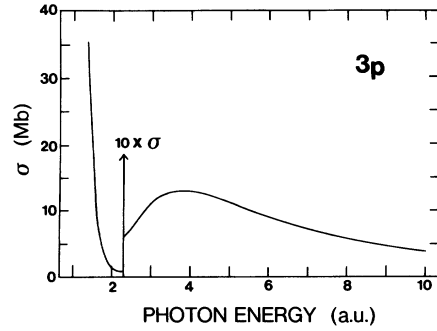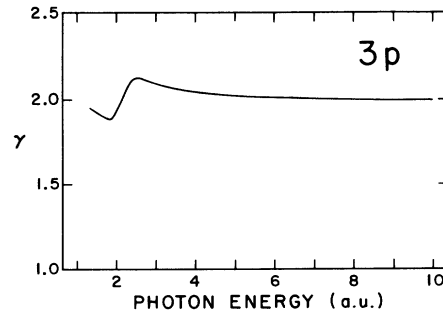

FIG. 3. Branching ratio for the 3p subshell.

two subshells. The present relativistic calculation gives some deviation from this statistical ratio in the near-threshold region as shown in Fig. 3. The variation of the branching ratio in the vicinity of the threshold is analogous to that occurring in argon.[16] The branching ratio starts out at a value below the statistical ratio near the $3p_{1/2}$ threshold but as the photon energy passes through the "Cooper" minimum region (which occurs at about 2.2 a.u.) for the $3p$ shell, γ increases rapidly above the statistical ratio. As the photon energy increases still further, the branching ratio gradually drops to the statistical ratio. This happens because the $3p_{3/2}$ subshell cross section reaches its Cooper minimum at an energy lower than that for the $3p_{1/2}$ subshell, and starts increasing while the cross section for $3p_{1/2}$ is still low.

The present RRPA calculations and the RPAE (Ref. 23) results practically coincide also for the $3s$ cross section over the energy range for which the RPAE results are reported. This is not surprising since the relativistic effects on the $3s$ cross sections are not expected to be significant. The partial cross section for the $3s$ subshell is shown in Fig. 4.

The angular distribution asymmetry parameter $\beta_{n\kappa}$ for photoionization from the $4s$, $3p$, and $3s$ has also been investigated in the present study. Unfortunately, no experimental data on this interesting parameter are available. Nonrelativistically, β_{ns} should be equal to 2 and independent of energy.[24] However, due to relativistic dipole transitions to the triplet states, deviations of β_{ns} from 2 can occur.[17] In the present calculations, β_{ns} has been found to be equal to 2 for the $4s$ and $3s$ shells over the entire energy range above the $3p_{3/2}$ threshold (except for the $4s$ shell in the autoionizing region below the $3p_{1/2}$ threshold) thus demonstrating a nonrelativistic behavior. The asymmetry parameter for the $3p$ subshell is shown in Fig. 5 and has been obtained from $\beta_{3p_{3/2}}$ and $\beta_{3p_{1/2}}$ by taking the weighted average

$$\beta_{3p} = \frac{\sigma_{3p_{3/2}}\beta_{3p_{3/2}} + \sigma_{3p_{1/2}}\beta_{3p_{1/2}}}{\sigma_{3p_{3/2}} + \sigma_{3p_{1/2}}} . \tag{4}$$

The variation in the vicinity of the Cooper minimum for the $3p$ shell is significant here due to interference between the $3p\rightarrow s$ and $3p\rightarrow d$ amplitudes.

III. SPIN POLARIZATION

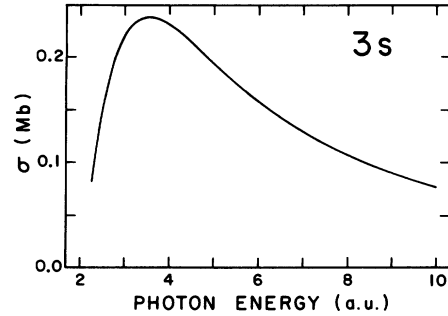It has been established both theoretically and experimentally that polarized electrons can be ejected

FIG. 4. $3s$ subshell cross section.

from unpolarized atoms by unpolarized radiation.[25,26] Nonrelativistic theory predicts no spin polarization nonrelativistically for the np shell since the polarization from the $np_{3/2}$ and $np_{1/2}$ subshells would be in a ratio of 1:2 which is completely offset by the corresponding ratio of partial cross sections.[27,28] In reality (and in relativistic theory) net spin polarization does occur even for photoionization from the ns subshell due to the spin-orbit interactions which lead to interference between the dipole amplitudes for the $ns\rightarrow p_{3/2}$ and $ns\rightarrow p_{1/2}$ channels. The spin polarization is expressed in terms of dynamical parameters (ξ,η,ζ,δ) which are in turn given as weighted sums of dipole matrix elements.[29,30] Using RRPA amplitudes, the components of the spin-polarization vector are predicted. The notations used are those of Huang.[29]

The spin-polarization parameters ξ, η, ζ, and δ are, respectively, proportional to the x,y,z components of the spin-polarization vector $\vec{P}$. Considering specifically the case of incident circularly polarized radiation one finds that

$$P_x = \pm\xi\sin\theta/F(\theta) , \tag{5a}$$

$$P_y = \eta\sin\theta\cos\theta/F(\theta) , \tag{5b}$$

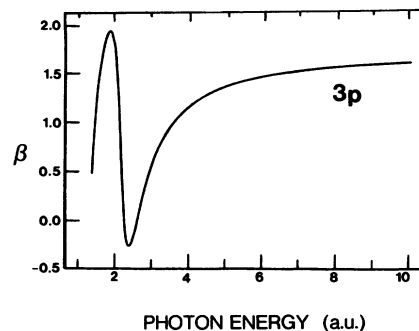$$P_z = \pm\zeta\cos\theta/F(\theta) , \tag{5c}$$

PHOTON ENERGY (a.u.)

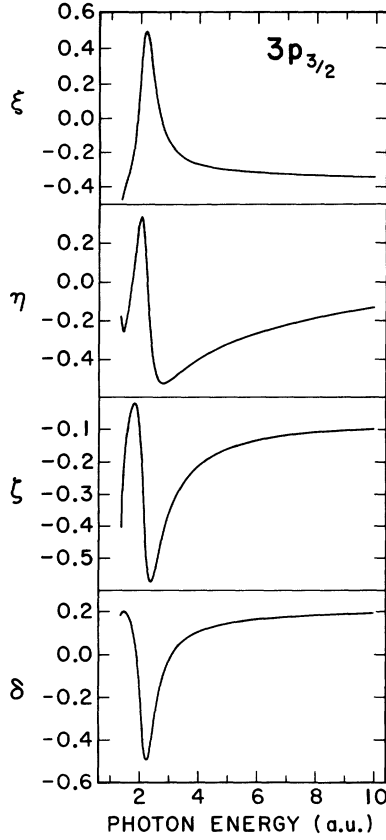FIG. 5. Asymmetry parameter for the $3p$ subshell.

FIG. 6. Spin-polarization parameters for the $3p_{3/2}$ subshell.

and

$$P_{\text{tot}} = \pm\delta , \qquad (5d)$$

where

$$F(\theta) = 1 - \tfrac{1}{2}\beta P_2(\cos\theta) \qquad (6a)$$

and

$$\delta = (\zeta - 2\xi)/3 . \qquad (6b)$$

The coordinate frame (x,y,z) is set up so as to have the z axis along the direction $\vec{p}$ of the outgoing electron, the y axis along $\vec{k} \times \vec{p}$, and the x axis along $[\vec{k} \times \vec{p}] \times \vec{p}$. The $\pm$ signs in the above equations refer to the helicity of the incident radiation being positive or negative.

The $4s$ and $3s$ spin-polarization parameters for calcium are found to be essentially zero except that the parameters for photoionization from the $4s$ subshell show slight departure from zero in the region of the autoionization resonances. The corresponding parameters for the $3p_{3/2}$ subshell are shown in Fig. 6. The parameters for the $3p_{1/2}$ subshell are similar in profile but opposite in sign and they ap-

proximately cancel the polarization parameters for the $3p_{3/2}$ subshell when weighted by their respective photoionization probabilities.

IV. AUTOIONIZATION RESONANCES

The RRPA shares a practical difficulty with other many-body theories in extracting information about highly excited bound states and resonances.[10] Typically, such resonances occur in the photoionization calculations because of coupling between interacting closed and open channels in the neighborhood of ionization thresholds. The multichannel quantum defect theory has been developed[2,3,18,31−33] to treat such coupled-channel problems in an efficient manner.

A. The $3s_{1/2} \rightarrow np_{1/2}$, $np_{3/2}$ resonances

For the analysis of the resonances below the $3s$ threshold, we consider the following seven interacting dipole channels:

$$3p_{3/2} \rightarrow s, d_{3/2}, d_{5/2} ,$$

$$3p_{1/2} \rightarrow s, d_{3/2} ,$$

and

$$3s \rightarrow p_{1/2}, p_{3/2} .$$

The $4s \rightarrow p_{1/2}, p_{3/2}$ channels are omitted as they have little influence in the resonance structure. The
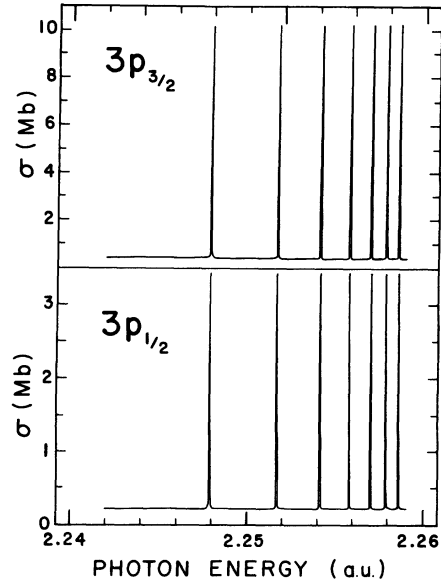

FIG. 7. Cross sections for the $3p_{3/2}$ and $3p_{1/2}$ autoionization resonances.

$3s \rightarrow p$ channels are closed for photoionization below the $3s$ threshold; in the absence of coupling, these two channels would lead to $3s \rightarrow np$ bound states converging to the $3s$ threshold. With coupling present, the $3s \rightarrow np$ states become autoionization resonances. The autoionizing resonances in the $3p_{3/2}$ and $3p_{1/2}$ cross sections are shown in Fig. 7. These resonances converge to the series limit at the $3s$ threshold, which occurs at 2.262 a.u. in the RRPA.

The asymmetry parameters and the spin-polarization parameters in the autoionization spectrum are of practical as well as academic interest and these are presented in Fig. 8 along with the cross sections on an effective quantum number (v) scale. It is interesting to note from Figs. 7 and 8 that the branching ratio γ for the background radiation in the autoionization resonance region is nearly equal to 2 but that γ rises to almost 3 near the resonances. This striking departure from the value 2 in the branching ratio at the resonances is due to the fact that the physically important channels near the autoionization region of the spectrum are not LS coupled[13,34] in the MQDT analysis. The spin-polarization parameters for the $3p_{3/2}$ and $3p_{1/2}$ resonances shown in Fig. 8 are however approximately

reflections of each other and jointly tend to cancel as the nonrelativistic theory predicts.

B. The $3p_{1/2} \rightarrow ns_{1/2}$, $nd_{3/2}$ resonances

We analyze the autoionization resonances between the $3p_{1/2}$ and $3p_{3/2}$ thresholds considering the following seven interacting channels:

$$4s \rightarrow p_{1/2}, p_{3/2} \, ,$$

$$3p_{3/2} \rightarrow s_{1/2}, d_{3/2}, d_{5/2} \, ,$$

$$3p_{1/2} \rightarrow s_{1/2}, d_{3/2} \, .$$

Here we omit the $3s \rightarrow p_{1/2}, p_{3/2}$ channels which are found to be unimportant. The two channels originating from $3p_{1/2}$ in this case are closed for photoionization below the $3p_{1/2}$ threshold. Again, interaction between the closed and open channels leads to autoionization resonances converging to the ionization threshold for the $3p_{1/2}$ level which occurs in the RRPA at 1.349 a.u. These resonances are shown in Fig. 9. The autoionization resonance spectrum in this energy range consists of two resonant series: a sharp series associated with $3p_{1/2} \rightarrow s$ resonances and a diffuse series associated with $3p_{1/2} \rightarrow d_{3/2}$ states. The resonance profiles are similar to the Beutler-Fano[35,36] resonances in the rare-gas atoms, which have been analyzed previously using the relativistic MQDT.[37] The asymmetry parameter and the spin-polarization parameter in
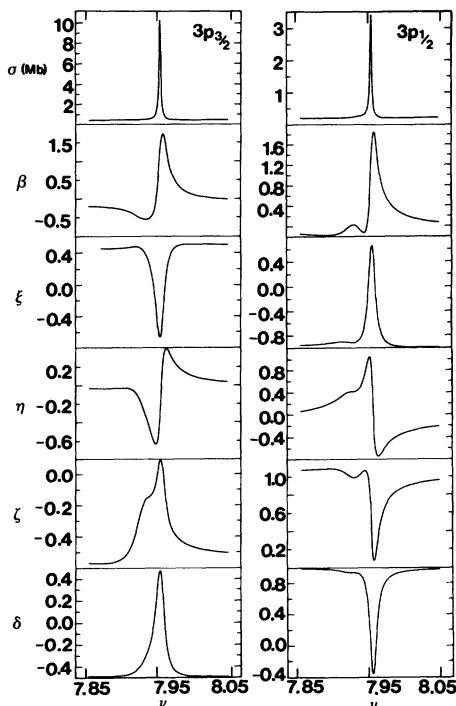
FIG. 8. Cross section, asymmetry parameter, and the spin-polarization parameters for the $3p_{3/2}$ and $3p_{1/2}$ autoionization resonances.
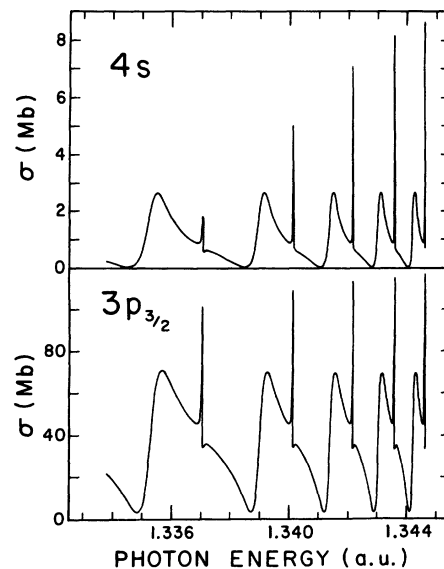
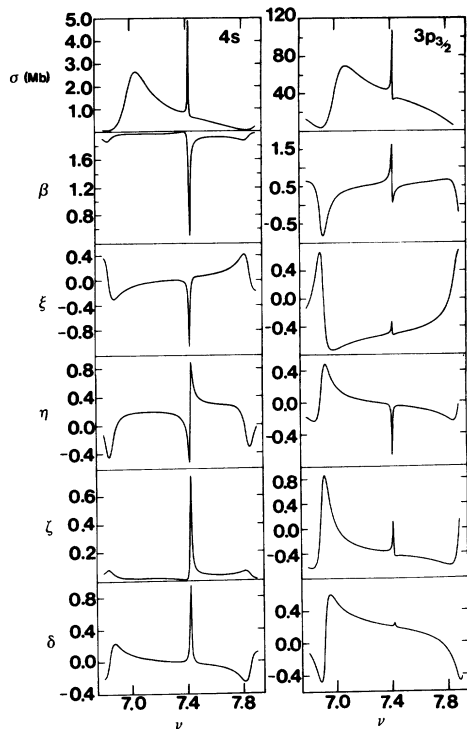FIG. 9. Cross sections for the $4s$ and $3p_{3/2}$ autoionization resonances.

FIG. 10. Cross section, asymmetry parameter, and the spin-polarization parameters for the $4s$ and $3p_{3/2}$ autoionization resonances.

the resonance region associated with excitation of both the $4s$ and $3p_{3/2}$ electrons are shown in Fig. 10 along with the cross section for these resonances.

V. PHOTOIONIZATION BELOW THE $3p_{3/2}$ THRESHOLD

We finally address ourselves to the question of photoionization from the $4s$ subshell below the $3p_{3/2}$ threshold. As mentioned in the introduction, this energy region is sensitive to configuration interactions and thus demands an analysis based on a multiconfigurational theory. However the prediction of a single-configurational theory is of some interest[23] and so the RRPA prediction for $4s$ cross section up to 1 a.u. from the threshold is shown in Fig. 11. The asymmetry parameter β for the $4s$ shell shows a dramatic departure from the value 2 near the Cooper minimum but the actual values of β obtained in this energy region are not of any practical interest due to the omission of the multiconfigurational interactions in the model employed in these calculations. Just as for the $3p$ and $3s$ subshells, the present results in the $4s$ cross section are almost identical to those of Amusia *et al.*,[23] since partial cross sections for calcium are insensitive to relativistic effects. The $4s$ cross section calculated
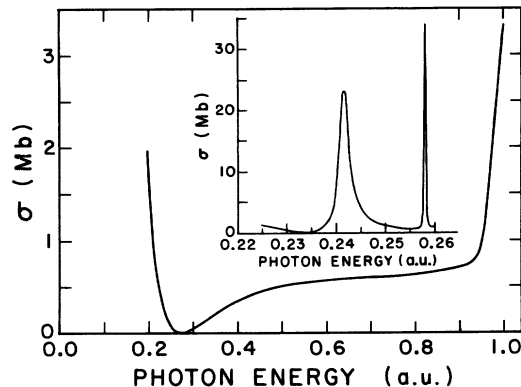

FIG. 11. $4s$ subshell cross section just above the threshold. The experimental curve of Ref. 8 is shown in the inset.

by McGuire[6] is lower than the RRPA and RPAE results; however, it goes through a Cooper minimum similar to that shown in Fig. 11 but at a slightly higher energy. The RRPA $4s$ cross section shows a dramatic rise near 1 a.u., due to interchannel coupling. The experimental cross section in this region[8] is shown in the inset of Fig. 11. The resonance peaks at 0.242 a.u. and at 0.258 a.u. in the experimental curve are due to $4s^2$:$^1S_0 - 3d\,5p$:$^1P_1^o$ and $4s^2$:$^1S_0 - 3d\,6p$:$^1P_1^o$ transitions, respectively.[7,10,12] Moreover, the $3dnp$:$^1P_1$ series is perturbed by the lowest members of the $4pns$:$^1P_1$ series.[3] These two electron correlations are not included in the RRPA.

VI. CONCLUDING REMARKS

The analysis in the paragraphs above is expected to provide a basis for the development of a multiconfigurational RRPA study of calcium. The present analysis in the energy region above the $3p_{3/2}$ threshold should be a useful guide for predicting the various physical photoionization processes since in this energy range the photoionization parameters are relatively less sensitive to multiconfigurational effects. Although calcium is a nonrelativistic atom, certain relativistic effects become important in the vicinity of the Cooper minima for the $4s$ and $3p$ subshells. The autoionization resonances below the $3s$ threshold demonstrate the breakdown of the LS coupling in the resonance region.

ACKNOWLEDGMENTS

*Present address: Department of Physics and Astronomy, Georgia State University, Atlanta, Georgia 30303.

[1]D. R. Bates and H. S. W. Massey, Proc. R. Soc. London Ser. A 177, 329 (1941).

[2]D. L. Moores, Proc. Phys. Soc. London 88, 843 (1966).

[3]J. Geiger, J. Phys. B 12, 2277 (1979).

[4]Y.-K. Kim and P. S. Bagus, J. Phys. B 5, L193 (1972).

[5]Y.-K. Kim and P. S. Bagus, Phys. Rev. A 8, 1739 (1973).

[6]E. J. McGuire, Phys. Rev. 175, 20 (1968).

[7]V. L. Carter, R. D. Hudson, and E. L. Breig, Phys. Rev. A 4, 821 (1971).

[8]R. D. Hudson and L. J. Kieffer, At. Data 2, 205 (1971).

[9]T. J. McIlrath and R. J. Sandeman, J. Phys. B 5, L217 (1972).

[10]W. R. S. Garton and K. Codling, Proc. Phys. Soc. London 86, 1067 (1965).

[11]V. J. Ehlers and A. Gallagher, Phys. Rev. A 7, 1573 (1973).

[12]M. W. D. Mansfield, Proc. R. Soc. London Ser. A 348, 143 (1976).

[13]M. W. D. Mansfield and G. H. Newsom, Proc. R. Soc. London Ser. A 357, 77 (1977).

[14]D. M. P. Holland and K. Codling, J. Phys. B 14, 2345 (1981).

[15]W. R. Johnson and C. D. Lin, Phys. Rev. A 20, 964 (1979).

[16]W. R. Johnson and K. T. Cheng, Phys. Rev. A 20, 978 (1979).

[17]W. R. Johnson, C. D. Lin, K. T. Cheng, and C. M. Lee, Phys. Scr. 21, 409 (1980).

[18]C. M. Lee and W. R. Johnson, Phys. Rev. A 22, 979 (1980).

[19]L. Carter and H. Kelly, J. Phys. B 11, 2467 (1978).

[20]W. R. Johnson, V. Radojevic, P. Deshmukh, and K. T. Cheng, Phys. Rev. A 25, 337 (1982).

[21]C. E. Moore, Atomic Energy Levels, Natl. Bur. Stand. (U.S.) Circ. No. 467 (U.S. GPO, Washington D.C., 1971), Vol. I.

[22]J. Cooper and R. N. Zare, J. Chem. Phys. 942 (1968).

[23]M. Ya. Amusia, and N. A. Cherepkov, Case Stud. At. Phys. 5, 47 (1975).

[24]U. Fano and J. W. Cooper, Rev. Mod. Phys. 40, 441 (1968).

[25]K. T. Cheng, K.-N. Huang, and W. R. Johnson, J. Phys. B 13, L45 (1980).

[26]U. Heinzmann, G. Schonhense, and J. Kessler, Phys. Rev. Lett. 42, 1603 (1979).

[27]N. A. Cherepkov, J. Phys. B 11, 1435 (1978).

[28]N. A. Cherepkov, J. Phys. B 12, 1279 (1979).

[29]K.-N. Huang, Phys. Rev. A 22, 223 (1980).

[30]K.-N. Huang, W. R. Johnson, and K. T. Cheng, Phys. Rev. Lett. 43, 1658 (1979).

[31]M. J. Seaton, Proc. Phys. Soc. London 88, 801 (1966).

[32]M. J. Seaton, Proc. Phys. Soc. London 88, 815 (1966).

[33]U. Fano, Phys. Rev. A 2, 353 (1970).

[34]U. Fano, J. Opt. Soc. Am. 65, 979 (1975).

[35]H. Beutler, Z. Phys. 93, 177 (1935).

[36]U. Fano, Nuovo Cimento 12, 154 (1935).

[37]W. R. Johnson, K. T. Cheng, K.-N. Huang, and M. Le Dourneuf, Phys. Rev. A 22, 989 (1980).